

Effect of Transmission Line Modeling Using Different De-embedding Methods

Ryo Minami, Changyo Han, Kota Matsushita, Kenichi Okada, and Akira Matsuzawa
 Department of Physical Electronics, Tokyo Institute of Technology
 2-12-1-S3-27, Ookayama, Meguro-ku, Tokyo, 152-8552, Japan
 Tel & Fax: +81-3-5734-3764
 Email: minami@ssc.pe.titech.ac.jp

Abstract—This paper discusses about device characterization for mmW transceiver design. Especially, the de-embedding error is evaluated with a 60 GHz 4-stage amplifier and measured data of transmission line. According to a comparison of characteristic impedances of transmission line which are derived by Thru-only and L-2L de-embedding methods, there are about 5.9% error at 60 GHz in Thru-only one and less than 1.7% error in L-2L one. The error is also evaluated with the 4-stage amplifier, and it results in 1.5 dB gain error and 2.6 GHz frequency shift.

I. INTRODUCTION

Recently, high-speed wireless communication at 60 GHz is attracted. This is because, the very wide bandwidth around 60 GHz can be used without license in many countries, and high speed wireless communications can be realized.

Moreover, since CMOS technology has been developed recently, it is possible to design RF frontend for 60 GHz by using CMOS instead of compound semiconductors. However, the parasitic capacitance and inductance affect the circuit performance seriously at 60 GHz. Thus, it is not so easy to realize accurate simulation for the mmW circuit design[1]. That's why more accurate de-embedding method and modeling technique are required.

In this paper, section II describes the RF frontend for mm-wave transceivers as an example, section III shows the accuracy of de-embedding method and modeling, section IV describes the effect of the model of transmission line (TL) which is used in each de-embedding method for a 4-stage power amplifier (PA).

II. CMOS RF FRONTEND FOR MM-WAVE TRANSCEIVERS

The authors have reported the first 16QAM direct-conversion transceiver for the 60 GHz wireless communication, which is implemented by using a 65 nm CMOS process[2]. Fig. 1 shows the block diagram of the transceiver and Fig. 2 shows the micrograph of chip.

The circuit of Rx consists of a 4-stage LNA, two mixers for IQ, and Quadrature Injection Locked Oscillator (QILO) for 60 GHz. From the point of view of power consumption, direct-conversion architecture is chosen. The local oscillator consists of 20 GHz Phase Lock Loop (PLL) and 60 GHz Injection Locked Oscillator (ILO).

The circuit of Tx consists of a 4-stage PA, two mixers for IQ, and QILO for 60 GHz which is the same with Rx. A direct-conversion architecture is also chosen for Rx.

Fig. 3 shows the constellation and performance summary. IQ modulated signals of 16QAM/8PSK/QPSK/BPSK are generated by using arbitrary waveform generator, and constellation is measured by using oscilloscope. The symbol rate is 1.76 Gs/s, and full-rate communication speed is possible for channel 1 and channel 2 of IEEE802.15.3c within a BER $< 10^{-3}$. The maximum data rates using wider bandwidth in QPSK and 16QAM with a 25% roll-off are at least 8 Gb/s and 11 Gb/s within a BER $< 10^{-3}$.

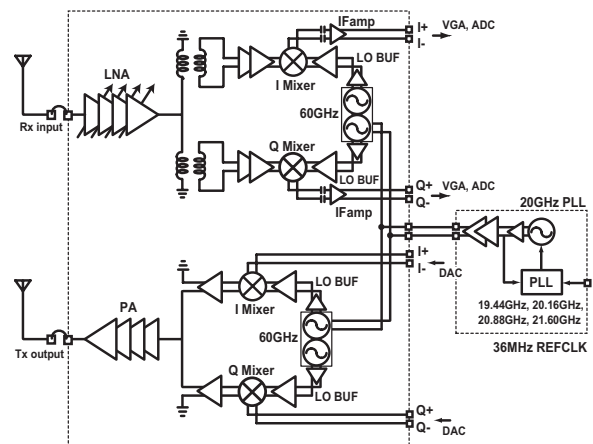


Fig. 1. Block diagram of the 60 GHz direct-conversion transceiver[2].

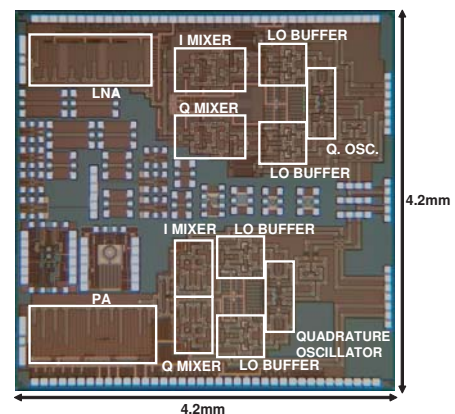


Fig. 2. Micrograph of chip[2].

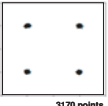
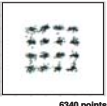
Constellation					
Modulation	BPSK	QPSK	8PSK	16QAM	
Data rate within 2.16GHz-BW	1.76Gb/s	3.52Gb/s (max 8Gb/s)	5.28Gb/s	7.04Gb/s (max 11Gb/s)	
EVM	-24dB	-28dB	-17dB	-17dB	
Distance (BER < 10 ⁻³)	0.5 – 274 cm	0.5 – 270 cm	0.5 – 20 cm	0.5 – 17 cm	
Tx	Rx		PLL		
CG	18.3dB	CG	17.3dB (high-gain mode)	Frequency	18 - 21GHz
P _{1dB}	9.5dBm		4.7dB (low-gain mode)	Phase Noise through Tx @60.48GHz	-95dBc/Hz
P _{SAT}	10.9dBm	NF	<6.8dB (high-gain mode)	Ref. spur	<-58dBc
PAE	8.8% (only for PA)	IIP3	-5dBm (only for LNA)	P _{out}	-2dBm
P _{DC}	186mW	P _{DC}	106mW	P _{DC}	66mW

Fig. 3. Measured constellation and performance summary[2].

III. TRANSMISSION LINE MODELING USING DE-EMBEDDING METHOD

At 60 GHz, the effect of parasitic capacitance and inductance is very large, which makes it difficult to obtain good matching between simulation result and measurement. Thus, it is required to improve the accuracy of simulation to design circuit more reliably.

Modeling of each active and passive devices, *e.g.*, transistor, transmission line, inductor, capacitor, balun, bend line, branch, pad, is very important to achieve fine simulation accuracy. One of the undesirable issues is that every parameters become frequency dependent at mmW frequency. For example, resistance depends on frequency due to the skin effect, and dielectric loss is also frequency dependent intrinsically. In addition, measurement is also very important to improve modeling accuracy.

To obtain accurate measurement data, de-embedding is one of the most important processes. The de-embedding is the process to remove the effects of test fixtures like probing pads. Probing pads are always required for high frequency measurements using probe stations. On the other hand, pads have very large parasitics at mmW frequency, and it is usually de-embedded to extract measured characteristics of intrinsic part like transistor, transmission line, etc.

Several de-embedding methods have been proposed so far. In this paper, open-short de-embedding method[3], thru-only de-embedding method[4], and L-2L de-embedding method[5] are evaluated.

Fig. 4 shows the structure of transmission line, which is a Guided Micro-Strip Line (GMSL). Fig. 5 shows the micrograph of TL, and 200- μm , 300- μm and 400- μm TLs are used for the evaluation. Fig. 6 shows the TL model used in this work, which has a separated for DC and AC characterization to model them respectively. In this work, attenuation constant α , phase constant β , quality factor Q , and characteristic impedance Z_0 are used to evaluate the

model accuracy. A circuit simulator (Agilent ADS) is used for parameter extraction.

A. Open-Short De-embedding Method

Fig. 7 shows α , β , Q , and Z_0 of the TL which is derived by the open-short de-embedding method. In this figure, each parameter has very large error over 20 GHz. One of the main reasons of this result is that the ideal short pattern cannot be achieved at high frequency because small parasitic components between signal pad and ground pad have to be considered. Thus, the data using the open-short de-embedding method cannot be used for modeling.

B. Thru-Only De-embedding Method

Fig. 8 shows α , β , Q , and Z_0 of the TL which is derived by the thru-only de-embedding method and TL model. The length of thru-line is 40- μm .

At high frequency, Z_0 is almost determined by inductance and capacitance. Thus, the TL model has to be carefully designed about inductance and capacitance. Moreover, α is mainly adjusted by conductivity, β is mainly adjusted by relative permittivity. The differences of the parameter between measured TL and TL model is less than 0.39% at 60 GHz. In this figure, the difference of parameters between 200- μm and 400- μm becomes larger at higher frequency. It is less than 5.89% at 60 GHz. The error is caused by the assumption that the thru-line can be characterized as a lumped-constant component. In this case, a 40- μm transmission line is used for the thru-only de-embedding. However, the 40- μm length cannot be regarded as a lumped-constant component at mmW frequency, and this results in the de-embedding error, which cannot be avoided theoretically[6].

In addition, the coupling between probes also influences on the measurement error. Probe coupling becomes larger

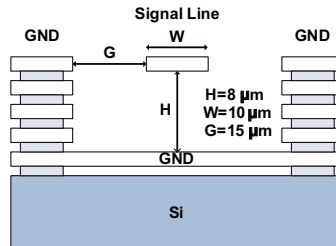


Fig. 4. The structure of TL.

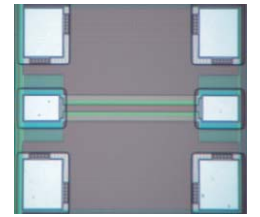


Fig. 5. Micrograph of TL.

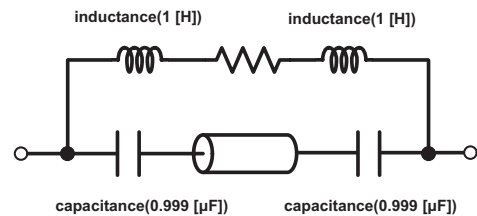


Fig. 6. Model of TL.

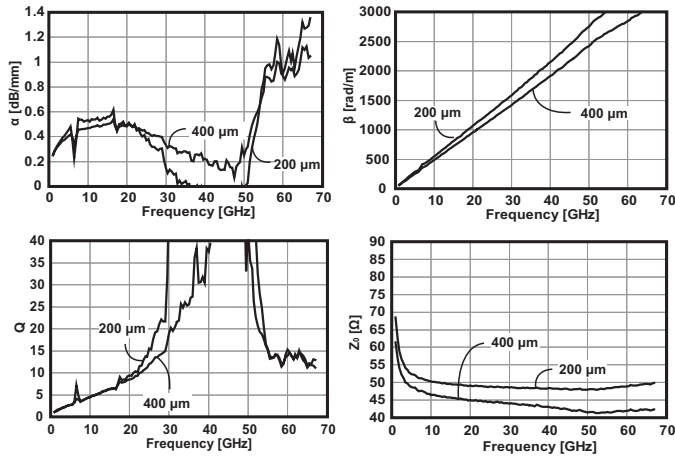


Fig. 7. TL using open-short de-embedding method.

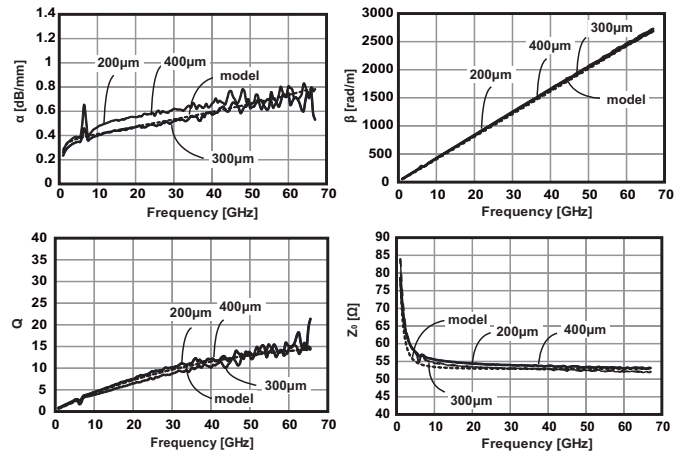


Fig. 9. TL using L-2L de-embedding method.

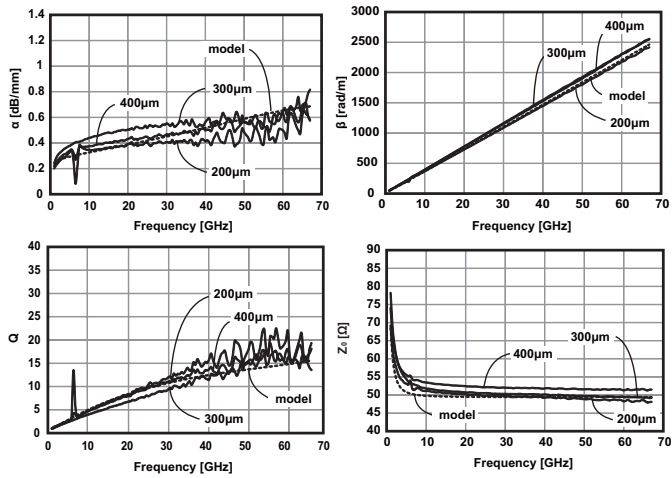


Fig. 8. TL using thru-only de-embedding method.

when the distance between probes becomes shorter. For a comparison, a TL model is characterized by using the average value of three TLs.

C. L-2L De-embedding Method

Fig. 9 shows α , β , Q , and Z_0 of the TL which is derived by the L-2L de-embedding method and TL model. In this figure, the differences of the characteristic impedance between measured TL and TL model is less than 0.35% at 60 GHz. Moreover, the parameters of 200- μm TL agree with 400- μm TL completely because these TLs and TLs using L-2L method are same. Thus the results of 200- μm TL and 300- μm are compared in this section. The error of characteristic impedance is less than 1.68% at 60 GHz. This is because L-2L de-embedding method does not use short pattern or thru-pattern which include the nonideal components such as parasitic capacitance and inductance. Thus, the L-2L method is theoretically more accurate than open-short and thru-only methods. Model parameters of TL are carefully extracted from these de-embedding data.

IV. 4-STAGE PA SIMULATION BY USING DIFFERENT TRANSMISSION LINE MODEL

To evaluate the accuracy of TL models, a 4-stage PA is designed. This PA is almost the same design with the circuit in [2]. The de-embedded results by the open-short method has very large error, so the de-embedded results by only the thru-only and L-2L methods are used for the evaluation. In this work, the evaluation is focused on about the accuracy of transmission line models, so the same models are used for transistor, T-junction, bend, decoupling MIM capacitor, and DC-cut series capacitor.

Fig. 12 shows a circuit schematic of the 4-stage PA, and it consists of the models explained above. Figs. 10 and 11 show simulated results of S_{21} , S_{11} , and S_{22} . There are 1.5 dB gain error and 2.6 GHz frequency shift in the simulated results using the thru-only and L-2L methods. According to the IEEE 802.15.3c standard, each channel has 2.16 GHz bandwidth, so this simulation error cannot be negligible.

Fig. 13 shows simulated results of large signal characteristics, and Table I summarizes the performance comparison. The simulation using the thru-only method has larger error for $P_{1\text{dB}}$ and PAE, which are 1.3 dB and 1.0%, respectively. Thus, simulation error of amplifiers depends heavily on the de-embedding methods, and the methods have to be carefully evaluated. In this work, the L-2L de-embedding method is employed to design the 60-GHz direct-conversion transceiver shown in Fig. 1.

V. CONCLUSION

This paper presents an evaluation of de-embedding methods for mmW transceiver design. The open-short de-embedding method has very large calculation error at more than 20 GHz, and it is infeasible to use the method for mmW device characterization. The thru-only de-embedding method is better than the open-short method. However, it still uses a lumped-constant model, and it results in large error at higher frequency such as 60 GHz. The characteristic impedance derived by the

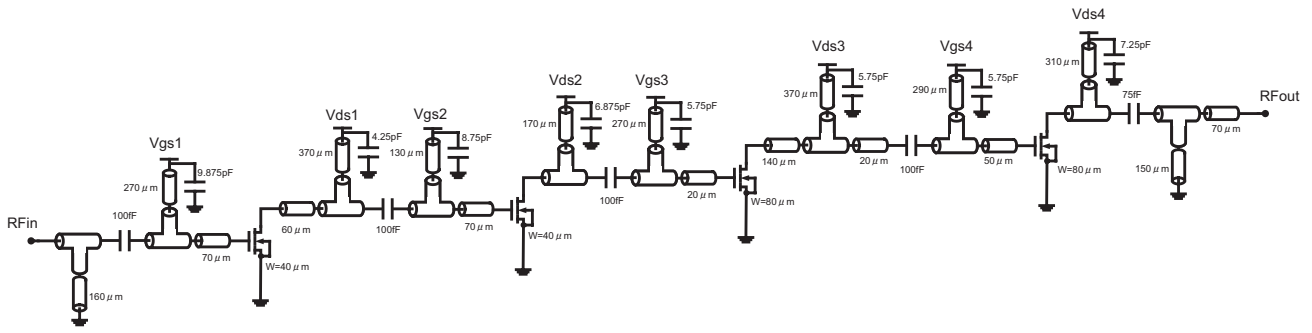


Fig. 12. Circuit schematic of 4-stage PA.

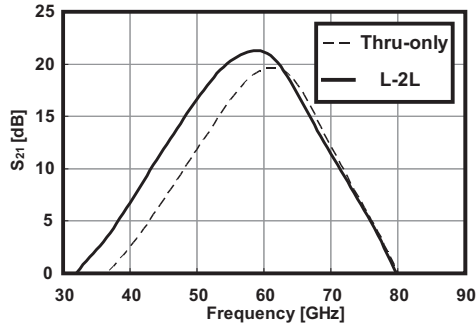


Fig. 10. Power gain.

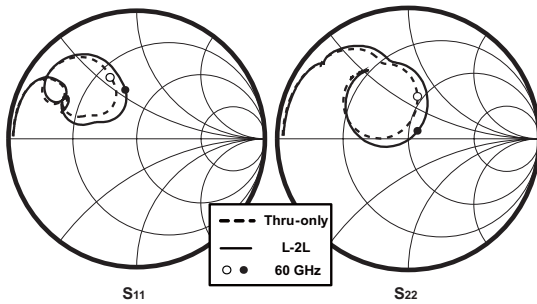


Fig. 11. S_{11} and S_{22} .

thru-only method have about 5.9% error at 60 GHz. The L-2L de-embedding method is the most accurate for transmission-line characterization, and the error is less than 1.7% at 60 GHz. The error is also evaluated with simulated results of the 4-stage amplifier using thru-only and L-2L models, and it results in 1.5 dB gain error and 2.6 GHz frequency shift. Especially, the error in P_{1dB} and PAE are critical as a power amplifier, which are about 1.3 dB and 1.0%, respectively. For an accurate device modeling, the L-2L de-embedding method is an indispensable technique for mmW circuit design.

ACKNOWLEDGMENT

This work was partially supported by MIC, SCOPE, MEXT, STARC, NEDO, Canon Foundation, and VDEC in collaboration with Cadence Design Systems, Inc., and Agilent Tech-

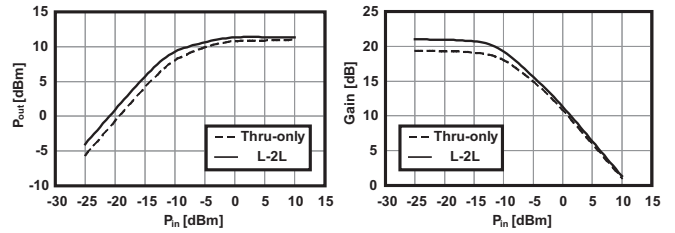


Fig. 13. Large-signal characteristic of 4-stage amplifier at 60 GHz.

TABLE I
PERFORMANCE COMPARISON.

	Thru-only model	L-2L model
Matching frequency [GHz]	61.4	58.8
Power gain [dB]	19.8	21.3
P_{1dB} [dBm]	7.41	8.78
P_{sat} [dBm]	11.0	11.4
Peak PAE [%]	6.51	7.45
Power consumption [mW]	169	170

nologies Japan, Ltd.

REFERENCES

- [1] K. Matsushita, N. Takayama, N. Li, S. Ito, K. Okada, and A. Matsuzawa, "CMOS Device Modeling for Millimeter-Wave Power Amplifiers," in *IEEE Radio-Frequency Integration Technology*, Dec. 2009, pp. 68–71.
- [2] K. Okada, K. Matsushita, K. Bunsen, R. Murakami, A. Musa, T. Sato, H. Asada, N. Takayama, N. Li, S. Ito, W. Chaivipas, R. Minami, and A. Matsuzawa, "A 60 GHz 16QAM/8PSK/QPSK/BPSK Direct-Conversion Transceiver for IEEE 802.15.3c," in *IEEE International Solid-State Circuits Conference Digest of Technical Papers*, Feb. 2011.
- [3] M. Koolen, J. Geelen, and M. Versleijen, "An improved de-embedding technique for on-wafer high-frequency characterization," in *Proceedings of the Bipolar/BiCMOS Circuits and Technology Meeting*, Sep. 1991, pp. 188–191.
- [4] H. Ito and K. Masu, "A simple through only de embedding method for on wafer s parameter measurements up to 110 GHz," in *IEEE MTT-S International Microwave Symposium Digest*, Jun. 2008, pp. 383–386.
- [5] J. Song, F. Ling, G. Flynn, W. Blood, and E. Demircan, "A de-embedding technique for interconnects," in *Electrical Performance of Electronic Packaging*, Oct. 2001, pp. 129–132.
- [6] N. Li, K. Matsushita, N. Takayama, S. Ito, K. Okada, and A. Matsuzawa, "Evaluation of a multi-line de-embedding technique up to 110 GHz for millimeter-wave CMOS circuit design," in *IEICE Transaction on Electronics*, vol. E93-A, no. 2, Feb. 2010, pp. 431–439.